Water Supply

IWA PUBLISHING

Water Supply Vol 22 No 3, 3498 doi: 10.2166/ws.2021.387

Study on applicability of remote sensing precipitation products in hilly-plain-wetland complex area of northeast China

Zhu-Xian Wang [a], Zi-Yang Wang [b,*], Peng Feng [a], Yang Dong [a], Zhao-Wei Zhang [a] and Ying-Kui Yang [a]

[a] Heilongjiang Provincial Meteorological Data Centre, Harbin 150030, China
[b] Heilongjiang Provincial Meteorological Service Center, Harbin 150036, China
*Correspondence author. E-mail: hljqxfwzx@163.com

Z-XW, 0000-0001-7029-6626

ABSTRACT

For the hilly-plain-wetland complex ecosystem in the cold region of Northeast China, in order to solve the problems, which include the scarcity of surface rainfall stations and the inability to provide accurate surface precipitation for hydrological process simulation, based on the observed precipitation of rainfall stations, three remote sensing precipitation products are taken as objects of evaluation. They include TRMM (Tropical Rainfall Measuring Mission) 3B42V7,3B42RT and CHIRPS (Climate Hazards Group InfraRed Precipitation with Station data, CHIP). In this paper, the observation data of rainfall stations and IDWP precipitation data interpolated by IDW (Inverse Distance Weighted) are used as true value of precision comparison, and the detection accuracy of remote sensing precipitation products from 2001 to 2010 is evaluated on the time scale (day, month and quarter) and spatial scale in Naoli River Basin.The results of the study indicated that 3B42V7 and CHIP have a high detection accuracy for precipitation, and their CC (correlation coefficient) values are 0.47 and 0.49 respectively in daily time scale. The accuracy of their observation for monthly precipitation is better than that of daily precipitation, and the CC are 0.85 and 0.87 respectively. The multi-year average precipitation at different grid positions in the basin is overestimated by 3B42RT, and its evaluation results are poor at different time scales. For the precipitation intensity range of (0,20], the observed results of 3B42V7 and rainfall station are close to each other. For the precipitation intensity ranges of (0,1) and (50,+∞), 3B42RT and CHIP have overestimated or underestimated the precipitation in different degrees. Based on the above analysis results, 3B42RT can be considered as data that can detect whether precipitation occurs on different spatial positions in the basin. 3B42V7 and CHIP can be applied to flood forecasting and non-point source pollution control in cold regions.

Key words: hilly-plain-wetland, Naoli River, remote sensing precipitation, spatial scale, time scale

HIGHLIGHTS

- The research area of this paper is a hilly-plain-wetland complex ecosystem, and its climate state is complex, so there are few studies on this research area.
- This paper studies the change of remote sensing precipitation with topography.
- This paper makes a statistical analysis of the error changes of remote sensing precipitation

1. INTRODUCTION

Precipitation is the basic meteorological and hydrological element of climate and terrestrial hydrological cycle system, and the temporal and spatial variation of precipitation will have great influence on surface runoff and water flow state (Jiang *et al.* 2016). Therefore, accurate observation of precipitation plays an important role in regional and global water resources management, climate change research, hydrological process simulation, drought and flood forecasting (Yong *et al.* 2010). For the precipitation data in the area with data, a certain number of meteorological and rainfall automatic observation stations are installed in the area, but the density of the station network is often low, which can only reflect the precipitation changes at the location of each station and its surroundings, but can not reflect the spatial precipitation changes in the region and large-scale basin (Wang *et al.* 2021). In areas where there is no or lack of data, especially in remote mountainous areas and deserts which are difficult to reach, the influence of these geographical factors often causes great limitations in precipitation

observation (Tan *et al.* 2015). In order to solve the above shortcomings of observations for surface precipitation, countries all over the world have launched meteorological satellites with different kinds of sensors, and adopted the data of different bands sent back to the ground by the sensors in real time and combined with the data of ground rainfall stations for correction, and developed different versions of real-time and delayed remote sensing precipitation products released after correction. Representative products include TRMM, CMORPH (The Climate Prediction Center Morphing Technique), CHIRPS and PERSIANN (precision estimation from remotely sensed information using artificial neural networks), etc (Li *et al.* 2015; Liu 2015a; Zhu *et al.* 2020), are widely used in various hydrological studies because they can provide high-precision and grid precipitation data of global continuous time series.

Before applying the above remote sensing precipitation data, it is very important to understand its data accuracy. Many studies have been carried out in areas such as plains, mountains and valleys (Jiang *et al.* 2012; Duan *et al.* 2016; Darand *et al.* 2017). For example, Liu (2015b) evaluated the difference of detection results of different magnitudes of precipitation by TRMMV6 and TRMMV7 on a global scale, and compared the detection accuracy on land and sea respectively; Mantas *et al.* (2015) evaluated the detection accuracy of TRMM 3B42V7 and TRMM 3B42RT in the Peruvian Andes; Wu *et al.* (2019) evaluated three precipitation products (CMFD, TRMM and CHIRPS) within a comprehensive framework, covering temporal and spatial consistency between the products, the errors of each product on the basis of extended triple collocation (ETC) analysis; Hu *et al.* (Li *et al.* 2012) compares the difference of TRMM with rain gauge data at different time scales and evaluates the usefulness of the TRMM rainfall for hydrological processes simulation and water balance analysis in the Xinjiang catchment. In the past, the research area selected by the previous research was single or relatively large in scale. However, there is less research on the complex ecological system. Wetland, as a transitional area for the exchange of materials between land and water, is sensitive to climate change, and climate change is also the main cause of degradation for wetland ecosystems. The uneven and unstable distribution of amount, frequency and intensity of precipitation in time and space affects the change of water content and area of wetland (Zhang *et al.* 2016). Accurate precipitation data is the basis for studying the impact of climate change on wetland ecosystems.

Based on the above discussion, the research purposes of this paper are as follows: taking the hourly precipitation of automatically observed by the surface rainfall station as the true value, the retrieval accuracy and spatial error distribution of the three satellite remote sensing precipitation products TRMM 3B42V7, TRMM 3B42RT and CHIRPS on the daily, monthly and quarterly time scale of 0.25× 0.25 degree and the spatial scale in the northeast alpine hilly-plain-wetland complex area are evaluated. This research can provide reliable precipitation data for the application of satellite remote sensing precipitation products in the region, and provide a reference method for the accuracy evaluation of more high-precision remote sensing precipitation products in the future.

2. STUDY AREA AND DATA SERIES

2.1. Study area

Naoli River Basin, located in the center of Sanjiang Plain in Heilongjiang Province, is one of the largest tributaries on the left bank of Wusuli River, and one of the most important areas for grain producing in China, with a total length of 596 km (Xing *et al.* 2018). The basin ranges from 131°31′E to 134°10′E and 45°43′N to 47°45′N, with sand dunes in the upstream and wet plains in the downstream. The watershed area extracted in this paper is 23,582 km^2, and the elevation ranges from 38 to 840 m (Xue *et al.* 2008; Mao *et al.* 2014). In order to evaluate the detection accuracy of remote sensing precipitation of each grid where rainfall stations are located, this paper encodes the remote sensing precipitation grid where rainfall stations are located. Taking 'A8G3' as an example, it indicates that there are three ground rainfall stations in the A8 grid. When evaluating the accuracy of grids with more than one rainfall station, the average value of precipitation in the grid is taken as ground reference precipitation data.

2.2. Data series

In this study, the ground reference precipitation data from January 1997 to December 2016 is collected from 14 rainfall stations in Naoli River Basin (Figure 1 and Table 1)., Satellite remote sensing precipitation products adopt TRMM 3B42V7 (Palomino-Ángel *et al.* 2019) (https://trmm.gsfc.nasa.gov/), TRMM3B42RT (Jiang *et al.* 2010) (https://trmm.gsfc.nasa.gov/) and CHIRPS (Cavalcante *et al.* 2020) (ftp://ftp.chg.ucsb.edu/pub/org/chg/products/CHIRPS-2.0/global_daily/tifs/p25/). The precision of remote sensing precipitation products is 0.25°× 0.25°. The reference precipitation data of spatial precision analysis adopts the measured precipitation data interpolated based on IDW method, and its precision is 0.25° × 0.25°. TRMM 3B42V7, 3B42RT, CHIRPS and raster precipitation data based on IDW interpolation are respectively referred

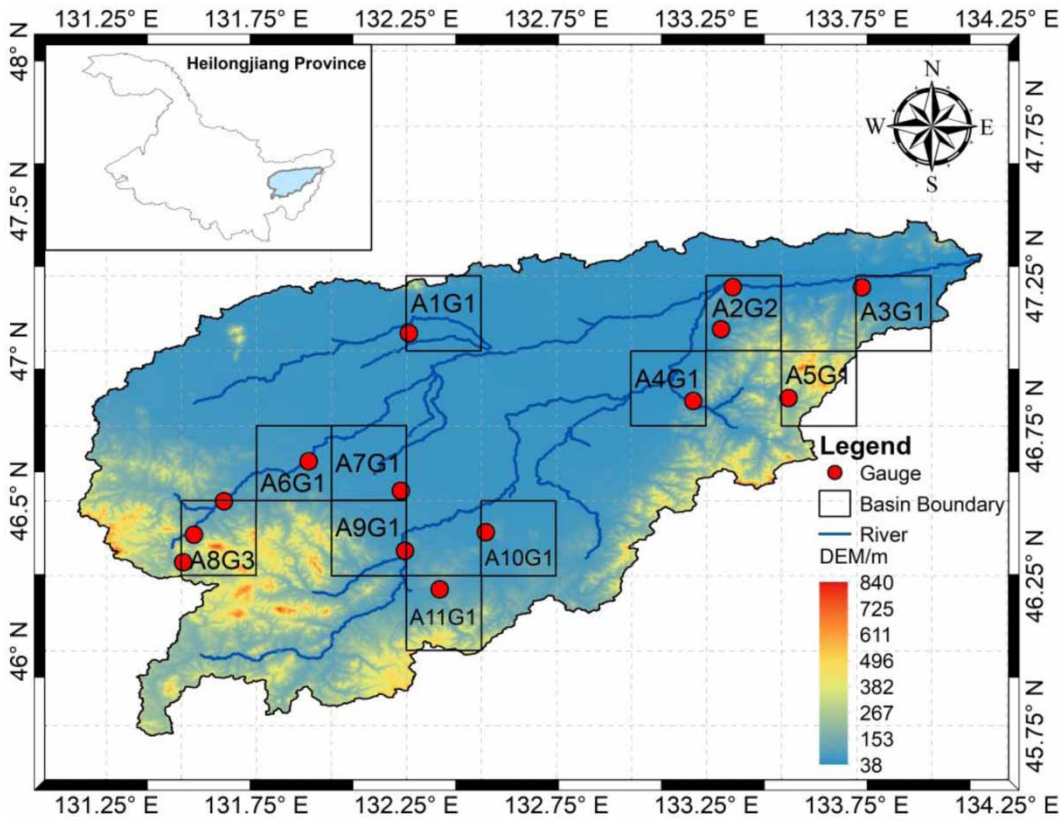

Figure 1 | The distribution map of study area.

Table 1 | Information on the rainfall stations which were collected in this study

Name	Longitude (°)	Latitude (°)	Annual average precipitation (mm)	Average monthly precipitation (mm)
Baoqing	132.25	46.33	525.6	43.8
Baoan	131.64	46.50	511.7	42.6
Benbeicun	132.23	46.53	460.3	38.4
Caizuizi	133.34	47.21	562.6	46.9
Dongfengcun	132.51	46.39	528.2	44.0
Hongqiling	133.21	46.83	532.6	44.4
Hongshengcun	132.36	46.20	455.0	37.9
Huaxincun	131.51	46.29	531.5	44.3
Qixinghezhen	131.92	46.63	480.6	40.1
Shichanglinchang	133.52	46.84	590.8	49.2
Toulincun	132.26	47.06	439.5	36.6
Xifenggoucun	133.30	47.07	556.7	46.4
Xiaojiahezhen	133.77	47.21	481.4	40.1
Yangmugangcun	131.54	46.39	527.2	43.9

to as 3B42V7, 3B42RT, CHIP and IDWP in this paper. The above raster data is processed by MATLAB, and the range of this remote sensing precipitation data is a global area. In order to improve the calculation speed of data, the raster data are read in batches by MATLAB, and are cut in batches according to the rectangular range of the outer boundary of the study area and

obtain remote sensing data with a smaller range. Then, the precipitation of the gauge is interpolated in batches at different times in this small range to obtain IDWP raster data. Finally, the two types of data correspond on the grid, and the precision of grid is 0.25° × 0.25°. The evaluation is obtained by index calculation of the values in the corresponding grid.

3. RESEARCH METHODOLOGY

In this study, the following indicators are used to quantitatively evaluate the accuracy of satellite remote sensing precipitation products in time and space scale (Yong *et al.* 2010; Nastos *et al.* 2016): correlation coefficient (CC), mean absolute error (MAE), root mean square error (RMSE), relative bias (BIAS), probability of detection (POD), false alarm rate (FAR) and critical success index (CSI). Their calculation formula is as follows:

$$CC = \frac{\sum_{i=1}^{n}(G_i - \overline{G})(R_i - \overline{R})}{\sqrt{\sum_{i=1}^{n}(G_i - \overline{G})^2}\sqrt{\sum_{i=1}^{n}(R_i - \overline{R})^2}} \tag{1}$$

$$MAE = \frac{1}{n}\sum_{i=1}^{n}|R_i - G_i| \tag{2}$$

$$RMSE = \sqrt{\frac{1}{n}\sum_{i=1}^{n}(R_i - G_i)^2} \tag{3}$$

$$BIAS = \frac{\sum_{i=1}^{n}(R_i - G_i)}{\sum_{i=1}^{n}G_i} \times 100\% \tag{4}$$

$$POD = \frac{U}{U + V} \tag{5}$$

$$FAR = \frac{W}{U + W} \tag{6}$$

$$CSI = \frac{U}{U + V + W} \tag{7}$$

where G_i is the precipitation of the rainfall stations; R_i is remote sensing precipitation; $\overline{G}$ is the average precipitation of the rainfall stations; $\overline{R}$ is the mean value of remote sensing precipitation; U is the numbers of hits; V is false alarm; W is the miss.

CC reflects the linear correlation degree between remote sensing precipitation and observed precipitation. MAE and RMSE reflect the average error of remote sensing precipitation. BIAS reflects the systematic bias error of remote sensing precipitation; POD reflects the underreporting degree of remote sensing precipitation products; FAR reflects the misreporting degree of remote sensing precipitation products; CSI reflects the proportion of successful observations of precipitation by remote sensing precipitation products. The values of CC, POD and CSI are close to 1 and the values of MAE, RMSE, BIAS and FAR are close to 0, which indicate that the detection accuracy of precipitation is high.

4. RESULTS

4.1. Influence of elevation on detection accuracy of remote sensing precipitation products

In order to understand the difference of detection accuracy of remote sensing precipitation products at different elevations, Figure 2 shows the relationship between the elevation of 11 coded grids and different evaluation indexes. It can be seen that the changed trends of different indicators for 3B42V7 and CHIP are roughly the same, and their average CC values are 0.47 and 0.49, respectively. The RMSE of 3B42RT is larger, but its BIAS at the maximum elevation is the lowest, which is 10%. The BIAS of 3B42V7 in each coding grid is lower. For the misreporting degree of precipitation events: 3B42RT > 3B42V7 > CHIP, the average values are 0.74, 0.39, and 0.33, respectively. In general, the detection accuracy of three remote sensing precipitation products did not change significantly with the increase in elevation.

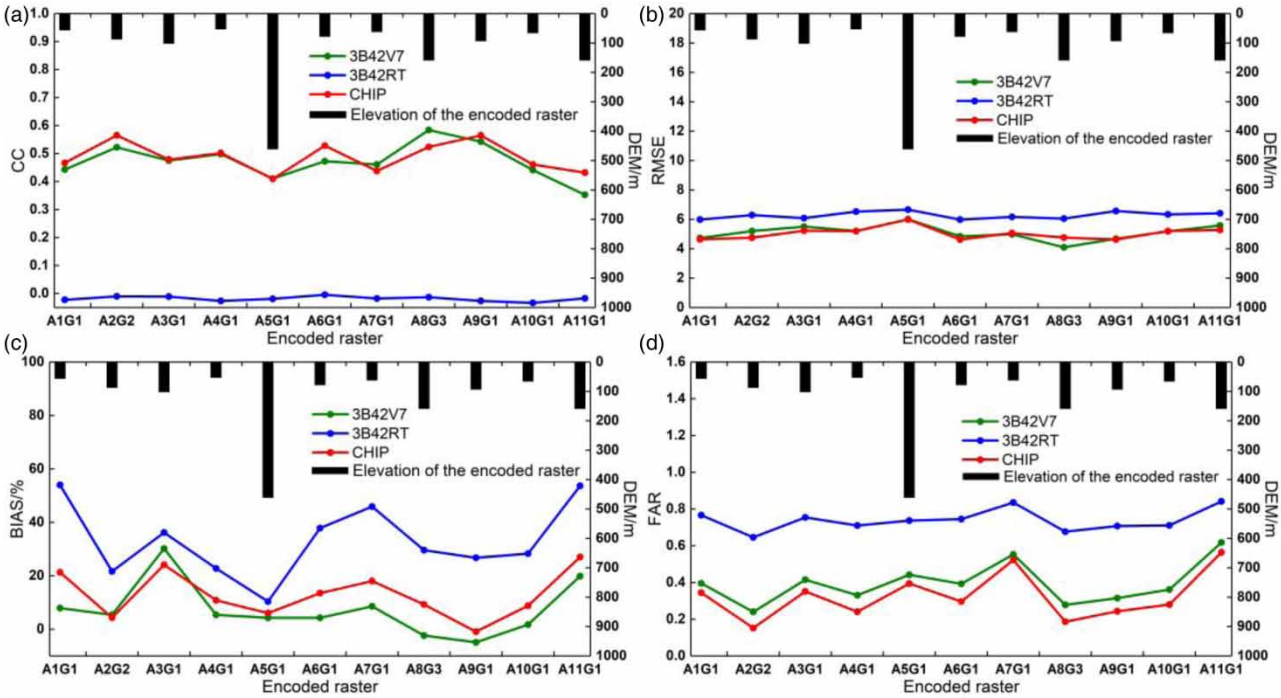

Figure 2 | The CC, RMSE, BIAS, FAR values of coded grids of different elevations.

4.2. The influence of GPCP/CAMS correction method on the detection accuracy of daily precipitation

In order to analyze the impact of the GPCP/CAMS (Fuchs *et al.* 2009) method on the daily precipitation after the TRMM monthly precipitation is corrected, the paper takes the average daily precipitation data of all grids and 14 rainfall stations in the basin as the daily average precipitation on the basin scale. The relative error of three remote sensing precipitation products is shown in Figure 3. It can be seen that the relative error of 3B42RT is relatively large, and the relatively large errors of the three remote sensing precipitation products mostly appear above the X axis. The maximum values of the absolute value for the relative error are 44.13 mm/d, 44.08 mm/d, and 58.10 mm/d respectively. This relative error shows alternate changes.

4.3. Analysis on the characteristic of the error variation of daily precipitation

To further illustrate the above problems, Table 2 shows the percentage of relative errors in the total number of days from 2001 to 2010 when the absolute error M of daily precipitation is greater than a certain threshold (1 mm/d, 3 mm/d, 6 mm/d). $n+$ and n− respectively represent the percentage of days whose absolute value of positive error and negative error are greater than a certain threshold to the total number of days, SRE+ and SRE− respectively represent the sum of positive error and negative error. Taking M greater than 1 mm/d as an example, the sum of the positive error and the negative error of 3B42RT is larger, and 3B42V7 is the smallest, and the values of the two errors are relatively close. This result shows that the positive and negative errors alternately cancel out each other. The sum of positive and negative errors of 3B42V7 and the sum of absolute errors are the smallest. The values are 281.4 mm/d and 3,738.7 mm/d respectively, which indicate that the detection accuracy of 3B42V7 is the best.

In order to further illustrate the accuracy of remote sensing precipitation, Table 3 shows the calculation results of statistical indicators of precipitation at different time scales for the 11 coded grids and surface rainfall stations in the basin. For daily time scale, the CC of 3B42V7 and CHIP are better, as they are 0.47 and 0.49 respectively, but compared with 3B42V7, the BIAS of CHIP is 12.29%, which is twice that of 3B42V7. CHIP overestimates the daily precipitation. The POD of the three remote sensing precipitations is relatively close, which is about 0.45, but the FAR of 3B42RT is higher, which is 0.74, and CHIP is the lowest, which is 0.32, and the correct ratio of observation of whether there is precipitation is the highest, as its CSI value is 0.39. For the monthly time scale, the CC of 3B42V7 and CHIP are both higher, as they are 0.85 and 0.87 respectively, and the

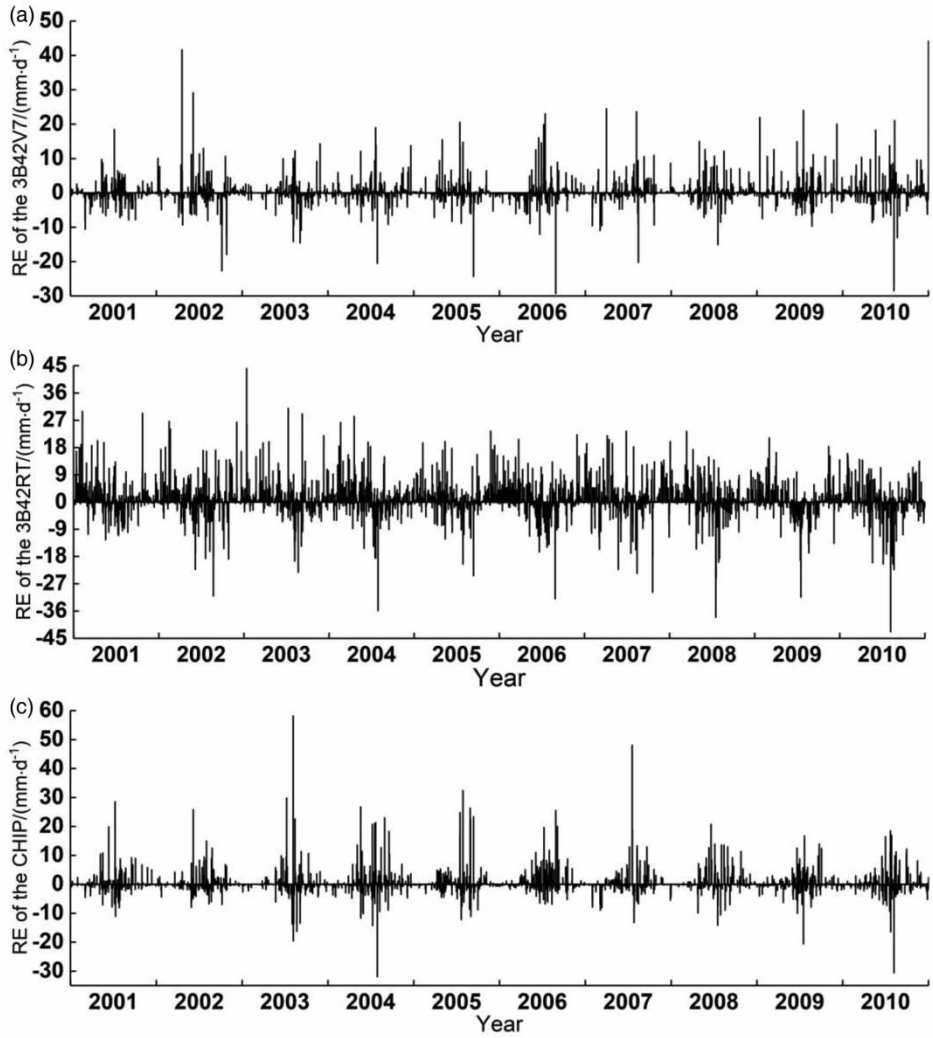

Figure 3 | Process line of daily average precipitation error in the basin scale.

Table 2 | Statistical results of daily precipitation error in basin scale

	M > 1 mm/d			M > 3 mm/d			M > 6 mm/d		
Prameters	**3B42V7**	**3B42RT**	**CHIP**	**3B42V7**	**3B42RT**	**CHIP**	**3B42V7**	**3B42RT**	**CHIP**
n_+/%	11.3	25.3	12.0	5.5	15.6	6.4	3.0	8.3	3.1
n_/%	13.3	20.0	13.2	5.1	10.7	4.8	2.1	5.6	1.8
$(n_+) + (n_-)$/%	24.6	45.2	25.1	10.6	26.3	11.2	5.0	13.9	4.9
S_{RE+}/mm	2,010.0	5,258.2	2,382.6	1,627.9	4,605.7	2,003.1	1,222.5	3,474.7	1,479.7
S_{RE-}/mm	−1,728.7	−3,761.3	−1,630.6	−1,179.9	−3,144.7	−1,083.3	−712.9	−2,344.4	−630.5
$(S_{RE+}) + (S_{RE-})$/mm	281.4	1,496.9	752.0	448.0	1,460.9	919.7	509.6	1,130.4	849.2
(S_{RE+})-(S_{RE-})/mm	3,738.7	9,019.6	4,013.2	2,807.8	7,750.4	3,086.4	1,935.4	5,819.1	2,110.2

observation accuracy of monthly precipitation is better. This is related to the correction of monthly precipitation which is corrected by the GPCP/CAMS method. In the quarterly period, the statistical indicators of 3B42V7 and CHIP are the same. Overall, the detection accuracy of 3B42V7 and CHIP is better, and the evaluation result of 3B42RT is poor.

Table 3 | Calculation results of 11 coding raster statistics indicators in the basin scale

Time	Types of data	Indicators of evaluation						
		CC	MAE (mm)	RMSE (mm)	BIAS	POD	FAR	CSI
Day	3B42V7	0.47	1.63	5.12	6.92%	0.46	0.39	0.35
	3B42RT	−0.02	2.78	6.28	32.10%	0.41	0.74	0.19
	CHIP	0.49	1.61	5.05	12.29%	0.48	0.32	0.39
Month	3B42V7	0.85	17.30	25.14	6.92%	0.90	0.01	0.90
	3B42RT	−0.20	44.49	56.29	32.10%	1	0.01	0.99
	CHIP	0.87	15.43	22.78	12.29%	0.99	0.01	0.98
Quarter	3B42V7	0.92	32.32	45.35	14.35%	1	0.00	1.00
	3B42RT	−0.14	108.44	141.79	47.12%	1	0.00	1.00
	CHIP	0.92	32.32	45.35	14.35%	1	0.00	1.00

4.4. Analysis of detection accuracy of different daily precipitation intensity

When the flood occurs, the different precipitation intensity will affect the flow rate of the surface water and the duration of the flood. In order to understand the proportion of different precipitation intensities for remote sensing precipitation products, there is targeted forecast for floods. The classification standard for the World Meteorological Organization is adopted in the study (Xing *et al.* 2018), and the daily precipitation is divided into a variation of 7 types of precipitation intensity. The frequency of the average precipitation of the grid at the basin scale is also calculated. Figure 4 shows a histogram stacked by percentage of daily precipitation frequency. With the increase of precipitation, the detection ratio of 3B42RT and rainfall station decreases gradually, and the observation results of 3B42V7 and rainfall station are closer at (0,20). Compared with the observation results of rainfall stations, 3B42RT overestimated by 24.14% at (0,1) and underestimated by 81.25% at (50, + ∞). On the contrary, CHIP is underestimated by 51.72% at (0,1), and 3B42V7 and CHIP are overestimated by 156.25% at (50, + ∞). 3B42RT is close to the rainfall station at (2,20).

4.5. Analysis of detection accuracy on the spatial scale of the basin

Influenced by topography and climate characteristics in different geographical locations, precipitation in different locations in the basin will have significant differences. In order to understand its distribution characteristics, Figure 5 shows the multi-year

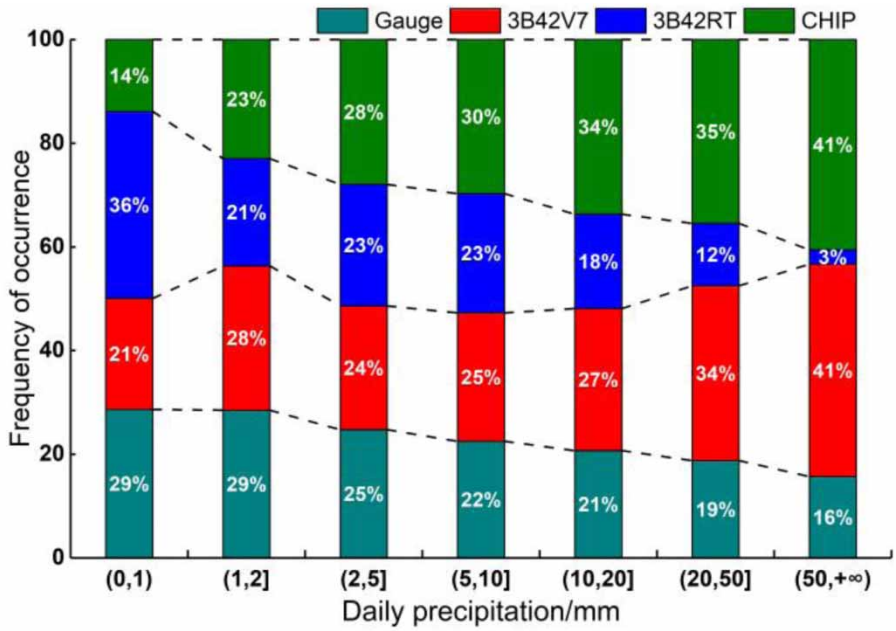

Figure 4 | Percentage stacking histogram of daily precipitation frequency at the basin scale.

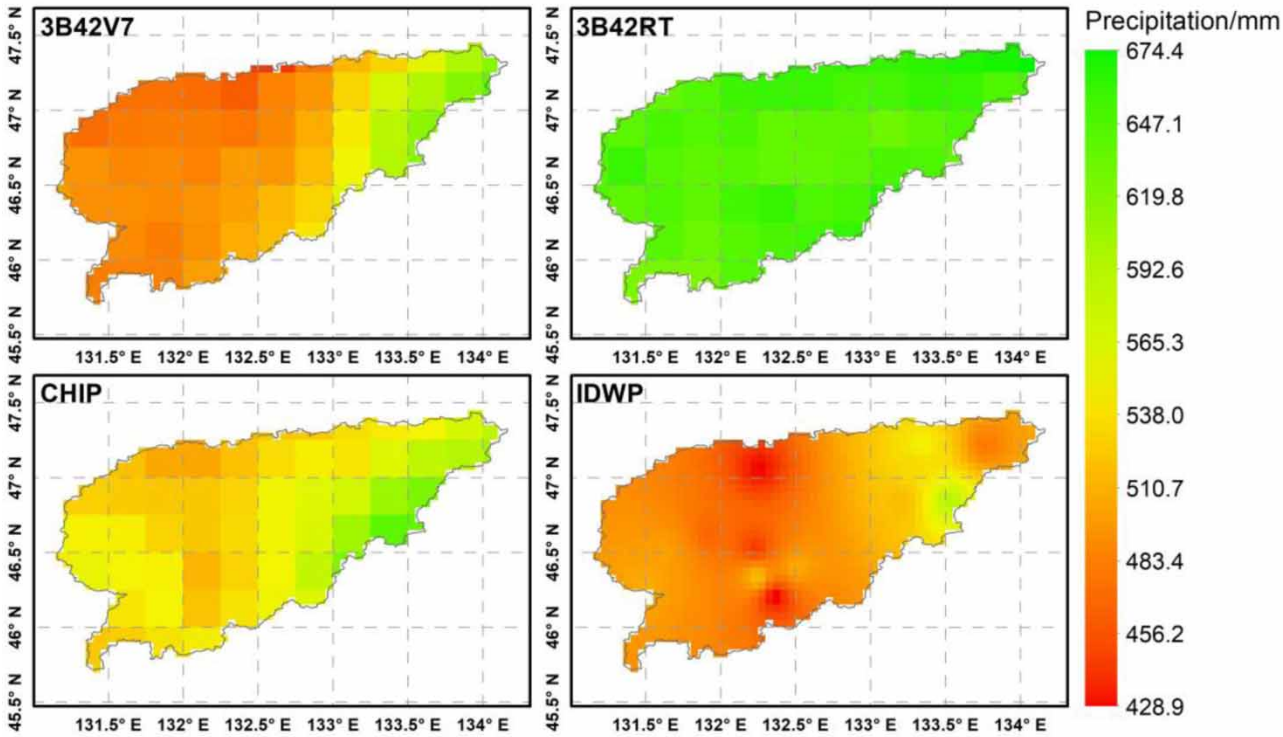

Figure 5 | Multi-year average precipitations of the basin.

average precipitation of three remote sensing precipitation products and IDWP. Compared with IDWP, 3B42V7 and CHIP overestimated the precipitation in the southeast of the basin, while 3B42RT in different grid locations overestimated the multi-year average precipitation, which varied from 621 mm to 674.4 mm.

In order to understand the detection accuracy of remote sensing precipitation products at different locations in the basin, Figure 6 shows the calculation results of each statistical index on the spatial scale of 0.05 ° × 0.05 ° cell size; it is indicated that the CC value of 3B42RT is low, but its CSI value is high, and the observed precipitation ratio is better than the other two precipitation products. 3B42RT can be considered as the basic data for detecting whether precipitation occurs at different locations in the basin. CHIP has higher detection accuracy for precipitation, and its spatial distribution of the CC value is better, while 3B42V7 only has higher detection accuracy in the southwest of the basin.

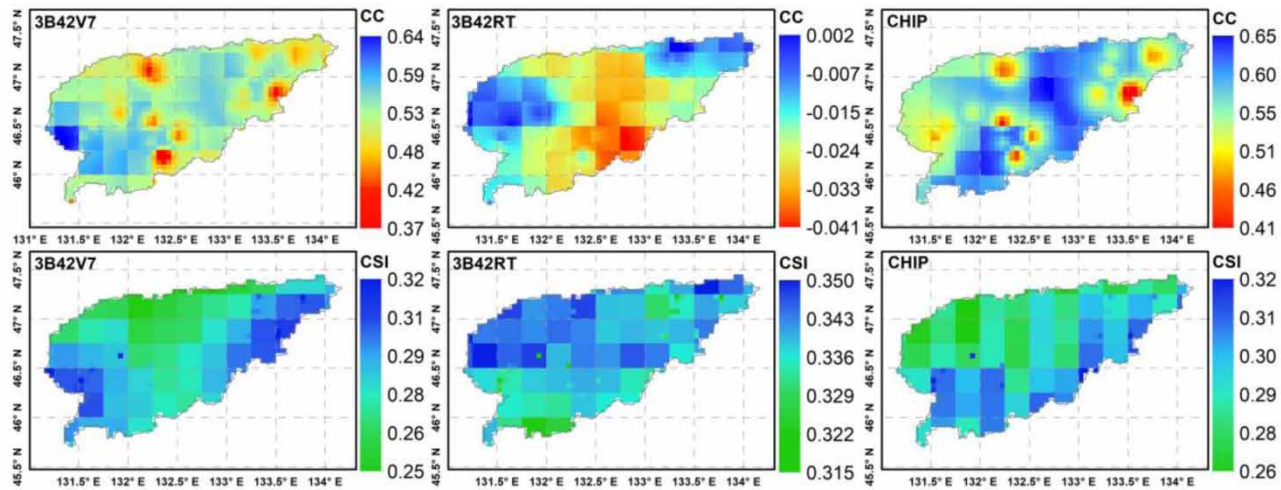

Figure 6 | Distribution map of statistical index for the spatial scale in the basin.

5. CONCLUSIONS

With the emergence of global precipitation products with high resolution and multi-sensor joint inversion, their ability to observe spatial precipitation has significantly improved. Taking a complex hilly-plain-wetland ecosystem as the study area, this paper evaluates the detection accuracy of three remote sensing precipitation products (3B42V7, 3B42RT and CHIP)at the time and spatial scales of day, month and quarter. The main conclusions of this study are as follows:

(1) In the complex area of hills-plains-wetlands, the detection accuracy of remote sensing precipitation products did not change significantly with the increase of elevation, and the relative errors of precipitation on the daily time scale mostly appeared above the X axis, and the relative errors changed alternately.
(2) The sum of positive errors and negative errors of 3B42RT is larger, and the sum of 3B42V7 is the smallest, and they are close to each other.
(3) The calculation results of statistical indicators for all coded grids on watershed scale indicated that the CC values of 3B42V7 and CHIP are better on daily time scale, but compared with 3B42V7, the BIAS of CHIP is relatively large, at twice that of 3B42V7, and the product overestimates the daily precipitation. On the monthly time scale, the CC values of 3B42V7 and CHIP are both high, and their observation effect on monthly precipitation is better, while the evaluation results of 3B42RT are poor.
(4) The analysis results at spatial scale indicated that 3B42RT overestimates the average annual precipitation at different grid locations, and CHIP has high detection accuracy for spatial precipitation.

According to the analysis results of this paper, 3B42RT can be used as the basic data to observe whether precipitation occurs in a complex hilly-plain-wetland area when the number of rainfall stations is insufficient and can not reflect the spatial change of regional precipitation. 3B42V7 and CHIP can be used as basic precipitation data for flood forecasting and non-point source pollution control in cold regions.

AUTHOR CONTRIBUTIONS

Z.X.W. completed the statistical analysis and wrote the paper; Z.Y.W., P.F., Y.D., Z.W.Z and Y.K.Y were responsible for study designing and modifying the language.

ACKNOWLEDGEMENTS

This paper was supported by National Key R&D Program of China (31671575).

CONFLICTS OF INTEREST

The authors declares that there is no conflict of interests regarding the publication of this paper.

DATA AVAILABILITY STATEMENT

Data cannot be made publicly available; readers should contact the corresponding author for details.

REFERENCES

Cavalcante, R. B. L., da Silva Ferreira, D. B., Pontes, P. R. M., Tedeschi, R. G., da Costa, C. P. W. & de Souza, E. B. 2020 Evaluation of extreme rainfall indices from CHIRPS precipitation estimates over the Brazilian Amazonia. *Atmos. Res.* **238**, 104879.

Darand, M., Amanollahi, J. & Zandkarimi, S. 2017 Evaluation of the performance of TRMM Multi-satellite Precipitation Analysis (TMPA) estimation over Iran. *Atmos. Res.* **190**, 121–127.

Duan, Z., Liu, J., Tuo, Y., Chiogna, G. & Disse, M. 2016 Evaluation of eight high spatial resolution gridded precipitation products in Adige Basin (Italy) at multiple temporal and spatial scales. *Sci. Total Environ.* **573**, 1536–1553.

Fuchs, T., Schneider, U. & Rudolf, B. 2009 The Global Precipitation Climatology Centre (GPCC) – in situ observation based precipitation climatology on regional and global scale. EGUGA **11**, 10519.

Jiang, S., Ren, L., Yong, B., Yang, X. & Shi, L. 2010 Evaluation of high-resolution satellite precipitation products with surface rain gauge observations from Laohahe Basin in northern China. *Water Sci. Eng.* **3**, 405–417.

Jiang, S., Ren, L., Hong, Y., Yong, B., Yang, X., Yuan, F. & Ma, M. 2012 Comprehensive evaluation of multi-satellite precipitation products with a dense rain gauge network and optimally merging their simulated hydrological flows using the Bayesian model averaging method. *J. Hydrol.* **452–453**, 213–225.

Jiang, S., Ren, L., Yong, B., Hong, Y., Yang, X. & Yuan, F. 2016 Evaluation of latest TMPA and CMORPH precipitation products with independent rain gauge observation networks over high-latitude and low-latitude basins in China. *Chinese Geogr. Sci.* **26**, 439–455.

Li, X.-H., Zhang, Q. & Xu, C.-Y. 2012 Suitability of the TRMM satellite rainfalls in driving a distributed hydrological model for water balance computations in Xinjiang catchment, Poyang lake basin. *J. Hydrol.* **426–427**, 28–38.

Li, H., Hong, Y., Xie, P., Gao, J., Niu, Z., Kirstetter, P. & Yong, B. 2015 Variational merged of hourly gauge-satellite precipitation in China: preliminary results. *J. Geophys. Res.* **120**, 9897–9915.

Liu, Z. 2015 Comparison of precipitation estimates between version 7 3-hourly TRMM multi-satellite precipitation analysis (TMPA) near-real-time and research products. *Atmos. Res.* **153**, 119–133.

Liu, Z. 2015 Comparison of versions 6 and 7 3-hourly TRMM multi-satellite precipitation analysis (TMPA) research products. *Atmos. Res.* **163**, 91–101.

Mantas, V. M., Liu, Z., Caro, C. & Pereira, A. J. S. C. 2015 Validation of TRMM multi-satellite precipitation analysis (TMPA) products in the Peruvian Andes. *Atmos. Res.* **163**, 132–145.

Mao, D., Wang, Z., Li, L., Song, K. & Jia, M. 2014 Quantitative assessment of human-induced impacts on marshes in Northeast China from 2000 to 2011. *Ecol. Eng.* **68**, 97–104.

Nastos, P. T., Kapsomenakis, J. & Philandras, K. M. 2016 Evaluation of the TRMM 3b43 gridded precipitation estimates over Greece. *Atmos. Res.* **169**, 497–514.

Palomino-Ángel, S., Anaya-Acevedo, J. A. & Botero, B. A. 2019 Evaluation of 3b42v7 and IMERG daily-precipitation products for a very high-precipitation region in northwestern South America. *Atmos. Res.* **217**, 37–48.

Tan, M. L., Ibrahim, A. L., Duan, Z., Cracknell, A. P. & Chaplot, V. 2015 Evaluation of six high-resolution satellite and ground-based precipitation products over Malaysia. *Remote Sens.* **7**, 1504–1528.

Wang, Q., Xia, J., She, D., Zhang, X., Liu, J. & Zhang, Y. 2021 Assessment of four latest long-term satellite-based precipitation products in capturing the extreme precipitation and streamflow across a humid region of southern China. *Atmos. Res.* **257**, 105554.

Wu, Y., Guo, L., Zheng, H., Zhang, B. & Li, M. 2019 Hydroclimate assessment of gridded precipitation products for the Tibetan Plateau. *Sci. Total Environ.* **660**, 1555–1564.

Xing, Z., Wang, Y., Ji, Y., Fu, Q., Li, H. & Qu, R. 2018 Health assessment and spatial variability analysis of the Naolihe Basin using a water-based system. *Ecol. Indic.* **92**, 181–188.

Xue, B., Keming, M., Liu, Y., Jieyu, Z. & Xiaolei, Z. 2008 Differences of ecological functions inside and outside the wetland nature reserves in Sanjiang Plain, China. *Acta Ecol. Sin.* **28**, 620–626.

Yong, B., Ren, L.-L., Hong, Y., Wang, J.-H., Gourley, J. J., Jiang, S.-H., Chen, X. & Wang, W. 2010 Hydrologic evaluation of multisatellite precipitation analysis standard precipitation products in basins beyond its inclined latitude band: a case study in Laohahe basin, China. *WATER Resour. Res.* **46**, W07542.

Zhang, Z., Wang, G., Jiang, M., Lu, X. & Liu, X. 2016 The impact of Holocene climate changes on Honghe wetland in NE China. *Ecol. Eng.* **96**, 72–78.

Zhu, B., Huang, Y., Zhang, Z., Kong, R., Tian, J., Zhou, Y., Chen, S. & Duan, Z. 2020 Evaluation of TMPA satellite precipitation in driving VIC hydrological model over the Upper Yangtze River Basin. *WATER* **12**, 550.

First received 4 June 2021; accepted in revised form 3 November 2021. Available online 15 November 2021